A hybrid neutron diffraction and computer simulation study on the solvation of N-methylformamide in dimethylsulfoxide

João M. M. Cordeiro and Alan K. Soper

Citation: The Journal of Chemical Physics **138**, 044502 (2013); doi: 10.1063/1.4773346
View online: http://dx.doi.org/10.1063/1.4773346
View Table of Contents: http://scitation.aip.org/content/aip/journal/jcp/138/4?ver=pdfcov
Published by the AIP Publishing

A hybrid neutron diffraction and computer simulation study on the solvation of *N*-methylformamide in dimethylsulfoxide

João M. M. Cordeiro[a] and Alan K. Soper
STFC Rutherford Appleton Laboratory, ISIS Facility, Harwell Science and Innovation Campus, Didcot, OX11 0QX Oxon, England

(Received 26 September 2012; accepted 11 December 2012; published online 24 January 2013)

The solvation of *N*-methylformamide (NMF) by dimethylsulfoxide (DMSO) in a 20% NMF/DMSO liquid mixture is investigated using a combination of neutron diffraction augmented with isotopic substitution and Monte Carlo simulations. The aim is to investigate the solute-solvent interactions and the structure of the solution. The results point to the formation of a hydrogen bond (H-bond) between the H bonded to the N of the amine group of NMF and the O of DMSO particularly strong when compared with other H-bonded liquids. Moreover, a second cooperative H-bond is identified with the S atom of DMSO. As a consequence of these H-bonds, molecules of NMF and DMSO are rather rigidly connected, establishing very stable dimmers in the mixture and very well organized first and second solvation shells. © *2013 American Institute of Physics*. [http://dx.doi.org/10.1063/1.4773346]

I. INTRODUCTION

Small molecules are important components of cellular solutions and play important roles in the protein folding and functioning. They are important in the control of protein denaturation[1] and its absence may be responsible for spurious aggregation of proteins.[2,3] Understanding the interactions between small molecules and how they associate with each other may be useful for understanding the binding of small biomolecules in solution and its influence on the self-assembly of larger functionally active biological molecules. The influence of dimethylsulfoxide (DMSO) on the peptide behavior is an interesting case of chaotropy/kosmotropy.[4,5] It has been shown that at moderate concentrations DMSO enhances enzyme activity (behaves as a kosmotropic agent) by increasing the conformational flexibility of the protein,[6,7] while in other cases the protein functionality was decreased (DMSO behaves as a chaotropic agent) by enhancing the protein rigidity.[8,9] Proteins dissolved in pure DMSO cannot exhibit functional activity because they become unable to adopt the native structure.[10] Experimental results suggest that DMSO denatures folded proteins by excluding water molecules from the protein surface.[11] Structural studies of DMSO as pure liquid and as a component of mixtures have been performed by diffraction as well as computational simulation.[12–20] It is a polar aprotic liquid widely used as organic solvent for both polar and nonpolar molecules with numerous applications in many branches of chemical and biochemical sciences.[21,22] Gaseous DMSO adopts a pyramidal C_s geometry by virtue of a lone pair of electrons present in sulphur with the SO polar group on an edge of the pyramid. The SO polar group can give rise to H-bond formation, while the two CH_3 groups can bring about hydrophobic effects.[23] *N*-methylformamide (NMF), on the other hand, contains the peptide bond in its structure and can act as proton donor and acceptor via its C=O and N–H groups and consequently form C=O···H–N hydrogen bonds (H-bond) to each other, the same type of H-bond that is known to play an important role in the stabilization of the ordered intramolecular structure of peptides and proteins in aqueous medium.[24] Moreover, these molecules also form the C–H···O=C weak H-bond, which is decisive in the stabilization of many biological systems, as has been reported.[25,26] Pure liquid NMF and its aqueous solutions have been the subject of study in recent years, both theoretically and experimentally.[27–34] Figure 1 shows a sketch of both molecules with the dipole moment vector indicated on them.

Recently, we started both experimental and theoretical investigations looking into the NMF–DMSO mixture.[35,36] This paper reports results obtained for a 20% NMF in DMSO mixture. The investigation was done using a hybrid experimental-theoretical approach: neutron diffraction with isotopic substitution (NDIS) is used to obtain experimental data on the mixture structure and empirical potential structure refinement (EPSR) simulations with Monte Carlo method are used to detail that structure. NDIS can provide structural information concerning inter-molecular interaction at an unparalleled level of detail at the atomic length scale (0–12 Å)[37–41] and through the coupling of that methodology with EPSR simulations, it is possible to extract pair-wise atomic interactions between a particular molecule and the surrounding solvent. The technique is highly informative in the investigation of the structure of many hydrogen bonded liquids.[42–45] The paper is organized as follows: in Sec. II it is outlined the neutron diffraction and the EPSR theory related to. In Sec. III the results obtained are shown and discussed and, finally, in Sec. IV it is summarized the main conclusions of the study.

[a]Author to whom correspondence should be addressed. Electronic mail: cordeiro@dfq.feis.unesp.br. Permanent address: Unesp - University Estadual Paulista, Depto de Física e Química, Av Brasil, 56, 15385-000, Ilha Solteira, SP, Brazil. Tel.: +55 18 3743 1064. Fax: +55 18 3742 4868.

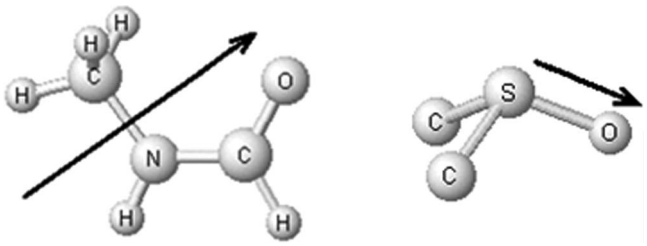

FIG. 1. NMF and DMSO molecules with the dipole moment vectors indicated on them. The hydrogen atoms of DMSO methyl groups were hidden for simplicity.

II. THEORY

A. Neutron diffraction

Neutron diffraction with isotopic substitution is the premier technique by which the structure of molecular liquids containing hydrogen can be determined.[19,46–48] This is primarily due to the lack of correlation between the atomic number and the strength of the nuclear scattering interaction where light atoms, such as hydrogen, have scattering intensities on the same order of magnitude as heavier elements.[49]

The quantity that is sought in any diffraction experiment is the structure factor, $S(Q)$, where Q, the magnitude of the change in the wave vector by the scattered neutrons is defined as $Q = \frac{4\pi}{\lambda}\sin\theta$. Here, λ is the wavelength of the incident neutrons and 2θ is the scattering angle. For powders, glasses, and fluids an immediate simplification is possible because $S(Q)$ and $g(r)$ then depend only on the magnitude of Q and r, respectively, and not on their directions. For a multi-component system, there is a partial structure factor $S_{\alpha\beta}(Q)$ term for each distinct pair of atomic types, α and β:

$$S_{\alpha\beta}(Q) = 1 + \frac{4\pi\rho}{Q}\int_0^\infty r(g_{\alpha\beta}(r) - 1)\sin(Qr)dr. \qquad (1)$$

$g_{\alpha\beta}(r)$ represents the real space correlations between pairs of atoms as a function of their separations, r, and is a primary aim of most structural studies of liquids and disordered materials. Although this is a one-dimensional integral, it is important to bear in mind that the diffraction experiments probe $S(Q)$ and $g(r)$ in three dimensions.

The sum of all partial structure factors weighted by the portion of atom type and scattering length of atoms present in the system comprises the total structure factor, $F(Q)$:

$$F(Q) = \sum_{\alpha\le\beta}(2 - \delta_{\alpha\beta})c_\alpha c_\beta b_\alpha b_\beta (S_{\alpha\beta}(Q) - 1), \qquad (2)$$

where c_α is the atomic fraction and b_α is the scattering length of isotope α.

Strictly, the quantity measured in a neutron experiment is the differential scattering cross section. In the absence of any corrections for attenuation, multiple scattering, and inelastic effects, the differential cross section is equal to the total structure factor, $F(Q)$.

In order to understand the average local structure of a liquid, integration of $g_{\alpha\beta}(r)$ (radial distribution function (RDF)) gives the coordination number (n) of atoms of type β around the atom α at the origin over the distance range r_1 to r_2:

$$n_\alpha^\beta(r) = 4\pi c_\beta \rho \int_{r_1}^{r_2} g_{\alpha\beta}(r) r^2 dr. \qquad (3)$$

In principle, $g(r)$ can be obtained by the trivial Fourier transform of $S(Q)$. However, such direct Fourier transforms will inevitably lead to a spurious structure in the calculated distribution due to the finite extent and statistical noise in the data.

B. Empirical potential structure refinement

Over the past decade, there have been significant advances in the methods of neutron diffraction with isotopic substitution. In practice, because of the limitations imposed by the availability of isotopes, it is usually not feasible to measure directly all of the partial structure factors and thereby all of the site-site RDFs present in the system. In order to obtain a full set of correlations for the systems studied, EPSR is used to model the diffraction data.[46,50,51] EPSR begins with a standard Monte Carlo simulation using an initial reference potential where the potential consists of an intramolecular harmonic potential to define the geometry of the molecules being modeled, and an intermolecular potential, which, in the present case, consisted of Lennard-Jones 12-6 potentials for the site-site interactions on different molecules as well as Coulombic interactions for some sites. This reference potential is used to generate a starting configuration of molecules. EPSR then iteratively adjusts a perturbation to this reference potential to obtain the best possible agreement between the computed $F(Q)$ and the experimental diffraction data. These perturbations are derived from the difference between the measured diffraction data and the corresponding functions calculated from the evolving simulation.[51] It is interesting to stress that the parameters of the reference potential are not altered during the simulations but the perturbation, that will constitute the empirical potential, is added to them during the simulations in such a way as to obtain a refinement in the structure. While EPSR provides a model which is consistent with the measured diffraction data, it does not necessarily provide the only possible interpretation of the experimental data.[19,50–52] Because of that it has so far proved impossible in EPSR to constrain both the energy and pressure in any reliable way such that the simulation is able to reproduce the correct thermodynamics of the system.[19] Thus, obtaining a fit to the measured data does not ensure the potential model is correct, but it is a necessary condition for any chosen potential model of the liquid. This direct comparison with the diffraction data in Q space is rarely done with conventional molecular dynamics and Monte Carlo simulations of molecular liquids. Once the structural model and associated perturbation potentials reach a satisfactory agreement with the experimental data, the simulation box can be used to extract structural information concerning the simulated intermolecular distributions.

TABLE I. 20%NMF-80%DMSO mixtures measured by neutron diffraction[a]

Samples	NMF	DMSO
N:D-D:D	$DCONDCD_3$	$(CD_3)_2SO$
N:HD-D:D	$HCONHCH_3/DCONDCD_3$[a]	$(CD_3)_2SO$
N:H-D:D	$HCONHCH_3$	$(CD_3)_2SO$
N:H-D:HD	$HCONHCH_3$	$(CH_3)_2SO/(CD_3)_2SO$[b]
N:H-D:H	$HCONHCH_3$	$(CH_3)_2SO$

[a]Notation: N:D–D:D≡NMF: fully deuterated-DMSO:fully deuterated. The meaning for the other 4 samples can be easily realized by analogy.
[b]The liquid is a mixture of 50% of the fully protonated and fully deuterated liquids.

III. EXPERIMENTAL

A. Neutron diffraction

The neutron scattering data were collected using the small angle neutron diffractometer for amorphous and liquid samples (SANDALS), located at the ISIS pulsed neutron source at the Rutherford Appleton Laboratory, Oxfordshire, UK. This instrument is optimized for the study of light element-containing liquids and glasses and, in particular, for hydrogen/deuterium isotopic substitution. The instrument concentrates its neutron detectors at scattering angles below 40°, which helps to reduce the effects of nuclear recoil when scattering neutrons from materials containing hydrogen. In addition to the detectors, SANDALS is equipped with a transmission monitor, which ensures the total cross section of the sample is measured over the range of wavelengths delivered by the incident beam. The system under analysis is a 20% NMF–DMSO mixture at ambient temperature about 25 °C. The pure liquids were purchased from Sigma/Aldrich chemical company and were used without further purification. Because neutrons scatter differently depending on the isotopes present in the measured material, a set of 5 chemically similar, but isotopically unique samples, was submitted to neutron scattering. Details of the samples' compositions are given in Table I.

Each sample was contained in a flat plate cell of internal dimensions 1 mm × 35 mm × 35 mm, constructed from $Ti_{0.68}Zr_{0.32}$ alloy with a wall thickness of 1.1 mm. With this alloy there is minimal coherent scattering contribution from the cell leading to a more tractable data analysis for the samples. The scattering data were analyzed using neutron wavelengths in the range $\lambda = 0.075$–3.5 Å over a corresponding Q-range for each dataset ranging from 0.1 to 30 $Å^{-1}$. After collection, the raw data were converted to $F(Q)$ using the program GUDRUN available at ISIS.[53] These routines correct the data for the contributions from the empty cell, instrument background, absorption, and multiple scattering and normalize the data to absolute units using the scattering of a vanadium standard. The remaining corrections to account for the contributions from inelastic scattering by the sample, which for protons can have a pronounced dependence on the scattering vector, Q, were performed using the "Top Hat" methods described recently.[53,54]

B. EPSR modeling

As outlined in Sec. II , the first action striving to analyze the data using EPSR is to take a suitable reference potential energy function that will be used as the seed to the subsequent structure refinement. A model previously optimized by one of us[27] was used for NMF and the P1 model optimized by Luzar and Chandler[19,20,55] was used for DMSO. The molecular geometries used were those reported previously.[19,27] In the simulations, all NMF molecules are the *trans* conformer, as previously discussed.[27] The potential between atoms α and β was represented by

$$U_{\alpha\beta}(r) = 4\varepsilon_{\alpha\beta}\left[\left(\frac{\sigma_{\alpha\beta}}{r}\right)^{12} - \left(\frac{\sigma_{\alpha\beta}}{r}\right)^{6}\right] + \frac{1}{4\pi\varepsilon_0}\frac{q_\alpha q_\beta}{r}, \quad (4)$$

where $\varepsilon_{\alpha\beta} = (\varepsilon_\alpha\varepsilon_\beta)^{1/2}$, $\sigma_{\alpha\beta} = 0.5(\sigma_\alpha + \sigma_\beta)$, the classical Lorentz-Berthelot mixing rules for the cross terms, and ε_0 is the permittivity of free space. The Monte Carlo simulation itself follows the traditional pattern,[56,57] with application of periodic boundary conditions, use of minimum image convention, and neighbor lists. The Lennard-Jones and the Coulomb potentials were truncated as described previously.[27]

Because the hydrogen bonded to nitrogen within NMF is labile, there is an isotopic exchange of hydrogens between the nitrogens in the 50% mixture of fully deuterated and fully protonated NMF (see Table I). This aspect has been taken into account in the isotopic weighting for the intermolecular correlations. The structure refinement was performed using an equilibrated cubic box with 100 NMF molecules and 400 DMSO molecules. For detailing the pair distribution energy and the dipole moment correlation, the simulation box has been scanned using a Monte Carlo protocol reported in Ref. 58.

IV. RESULTS AND DISCUSSION

Figure 2(a) shows the experimental total structure factors, together with the EPSR refined model fits obtained for the five samples listed in Table I. The overall quality of the fits is seen to be quite good, with only small discrepancies between the empirical EPSR model and the experimental data at low values of Q. As observed previously, the background and inelasticity corrections to the data are most difficult when the isotopomers contain light hydrogen (top to bottom in the plots).[40,41]

The total radial distribution functions, $f(r)$, that are obtained by direct Fourier transform of the inversion of the experimental structure factor data ($F(Q)$), and the corresponding functions calculated from the EPSR refined model are shown in Fig. 2(b). The fit is rather good in the range between about 1 Å and 3 Å, indicating that the molecular bonds in both components of the mixture are suitably represented. In particular, the good agreement in the region near 2 Å should be stressed, considering the need for an accurate characterization of the hydrogen binding between molecules, as has been pointed out previously.[41–44] The results shown in Fig. 2 suggest that the refined molecular models are able to mimic the intermolecular interactions in a reasonable manner. Thus, given that EPSR has achieved a molecular model which is able to reproduce the

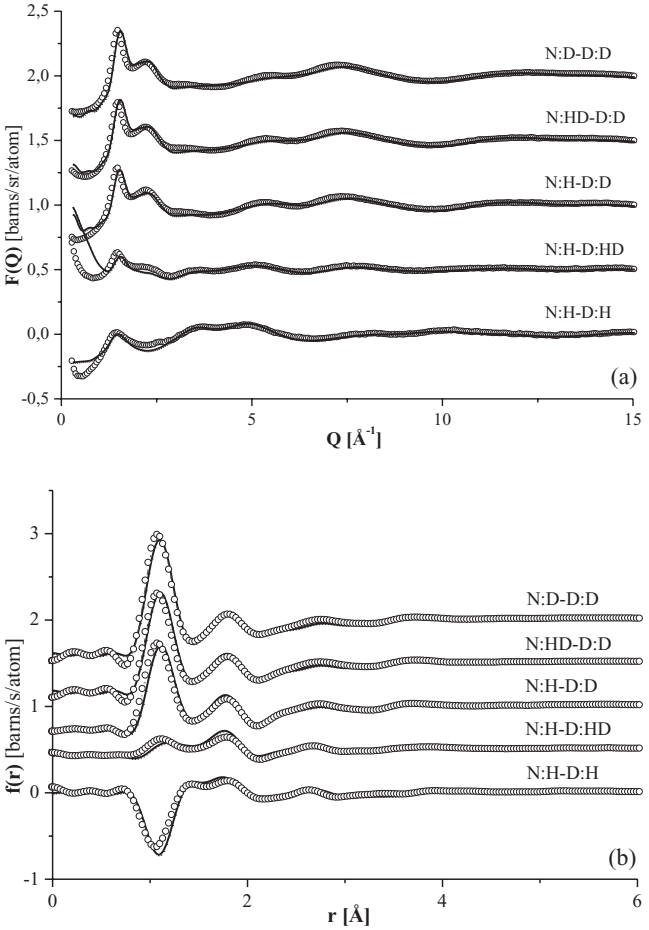

FIG. 2. (a) Experimentally measured total structure data (circles) and EPSR refined fits (solid line), and (b) composite radial distribution functions determined by direct Fourier transform of the experimental data (circles) and EPSR refinement (solid lines), for neutron scattering data collected on the samples listed in Table I. For clarity, the data for the different samples are shown shifted vertically by 0,5n, where $n = 0$, 1, 2, 3, and 4.

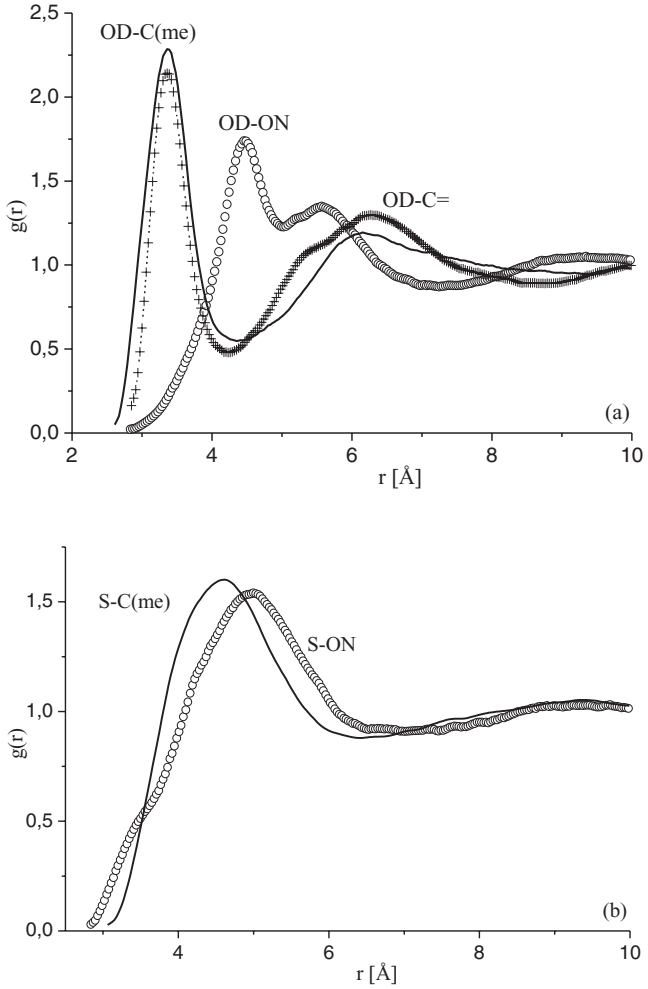

FIG. 3. Site-site radial distribution functions derived by the EPSR calculations for the atom pairs displayed in the figure. C(me) is the methyl carbon in NMF; C= is the carbonyl carbon in NMF, OD is oxygen in DMSO, ON is oxygen in NMF.

structure of the liquid, one might use the liquid simulations to further explore the intermolecular interactions. A natural starting point is to obtain the RDFs, $g(r)$, of DMSO–NMF correlations calculated from the EPSR refined model. Some of those RDFs are shown in Figs. 3 and 4 (for better understanding of the atomic symbols, see Fig. 1).

It can be seen that there is a pronounced correlation between some sites in DMSO and others in NMF, particularly the OD–C=, OD–C(me)N (Fig. 3(a)), and S–HN (Fig. 4(a)) correlations, suggesting a strong relative orientation of the molecules through the liquid. The OD–C= and OD–C(me)N peaks have amplitudes located around 3.4 Å, while the amplitude of the S–HN peak is located at 2.8 Å. These distances are remarkably short for these types of intermolecular correlations. Even a well structured second solvation shell can be perceived from these site-site correlations. But, more than that, the pattern of the OD–HN and OD–N $g(r)$'s shown in Fig. 4(b) is particularly interesting. Looking at the characteristics of the peaks one could immediately think of a H-bond forming between these two atoms. With a "bond length" of 1.6 Å the OD–HN correlation is even shorter than it is in other H-bonded liquids,[24] including water,[42,43,59] ethanol,[58] and NMF itself.[27,34] In the NMF–water mixture the O(H_2O)–HN peak is located around 1.9 Å.[60] These results point to a NMF–DMSO H-bond stronger than others found in classical H-bonded liquids and imply an extensive solvation of NMF molecules by DMSO. A comparison of these results with those reported previously for 80% and 50% concentrations[35] showed that the studied correlations are almost independent of the mixture concentration, since the amplitude and the position of the peaks are about the same. This invariance of the correlations with the concentration is ascribed to the strong interaction between the two liquids, strongly in line with the short distances of the correlations.

In Fig. 5 is shown the pair energy distribution from the simulation box for the intermolecular interaction between the NMF and the DMSO molecules, obtained using a protocol previously reported.[58]

As is standard in H-bonded liquids,[24] it is noted a first distribution of pairs, at very negative energy, attributed to the H-bonded pairs followed for a most likely set of pairs with energies in the range of about 0.0 and −2.0 kcal/mol. Nevertheless, different from other H-bonded liquids including pure water,[24] ethanol,[58] and the NMF itself,[34] the pair energy

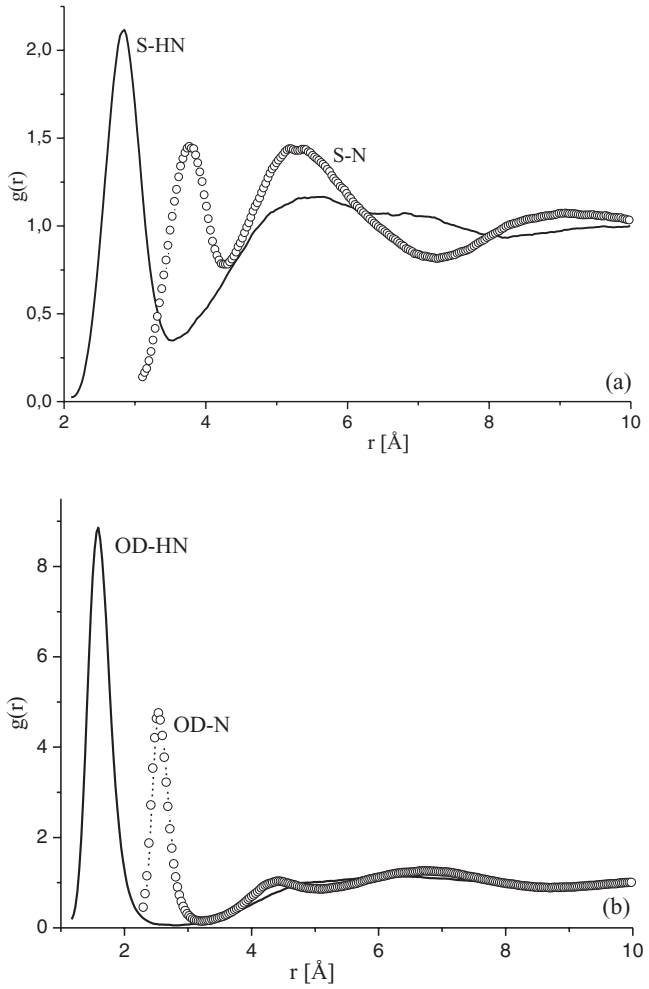

FIG. 4. Site-site radial distribution functions derived by the EPSR calculations for the atom pairs displayed in the figure. HN is the hydrogen bonded to nitrogen in NMF.

distribution of the NMF-DMSO mixture presents a shoulder around −5.5 kcal/mol, suggesting the presence of a particular kind of stable dimers in the mixture. Interestingly, the S–HN and S–N correlations shown in Fig. 4(a) present the same pattern of the OD–HN and OD–N correlations shown in Fig. 4(b), and associated with the H-bonding between NMF and DMSO molecules. These results suggest that a particular type of dimer, responsible for the S–HN and S–N correlations, is stable in the NMF-DMSO mixture, with energy distribution around −5.5 kcal/mol, which can also be associated with H-bonded pairs through the S atom. As the results indicate, these H-bonded molecules are less stable than the OD H-bonded ones, as it should be expected, considering the characteristics of the two different electronegative atoms concerned.

For better elucidating the detail of the liquid structure, the dipole-dipole correlation between the NMF and DMSO in the mixture was calculated using the same routine as above[58] and the $\langle \cos \theta \rangle$ (where θ is the angle between the vector of the molecular dipole moments of the two molecules under consideration) was plotted as a function of the distance between the molecules. The result is seen in Fig. 6 (see Fig. 1 for clearness). The distance between the molecules is, in fact, calculated measuring the distance between chosen atoms in

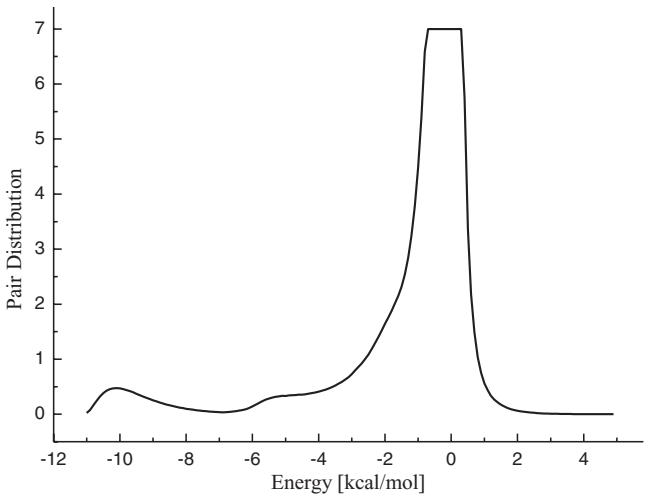

FIG. 5. Pair energy distribution in the simulation box (the pair distribution was limited to 7 for plotting).

each of the molecules (the atoms chosen in the present case are specified in the figure caption).

There is a strong dipolar correlation for C=–OD distances about 3.5 Å, with the molecules relatively positioned in such a way that the angle between the molecular dipole moment vectors is about 57°. Thus, at short distances the angle between the vectors of the molecular dipole moment is clearly fixed by the H-bonds between the molecules, while at larger distances the molecular correlation is mostly orientated for the dipole-dipole interactions. It is to be noted that both the pairs energy distribution (Fig. 5) and the dipole correlation (Fig. 6) are quite similar to the results reported for the 80% NMF mixture, while are different for those obtained for the 50% mixture.[35] The distribution of pairs through the energy of the 50% mixture is almost the double of those of the 20% and 80% mixtures. The comparison of the behavior of the dipoles orientation with the composition shows that the relative molecular orientation of the first solvation shell is invariant with the concentration. However, while the second solvation shell of the 80% and the 20% mixture presents the

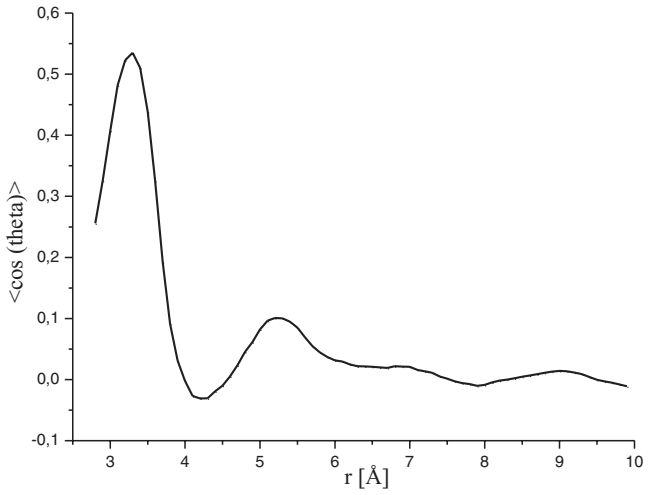

FIG. 6. Average dipole-dipole correlation as a function of the C=–OD distance.

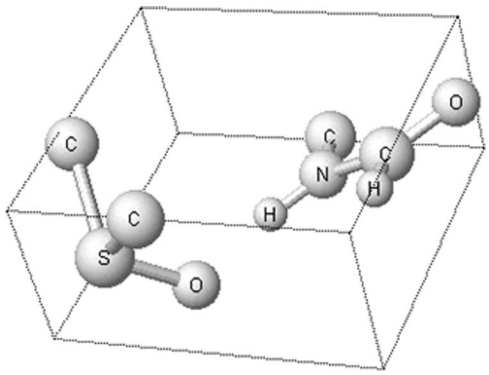

FIG. 7. The geometry of the most frequent NMF-DMSO dimer in the mixture (the hydrogen atoms of the methyl groups were hidden for simplicity). Geometric parameters: angles: (N–H···OD) = 168.9°, (N–H···S) = 151.3°, (S–O(D)···N) = 124.5°; distances: HN···OD = 1.53 Å, OD···C(me) = 3.52 Å, S···HN = 2.67 Å, N···OD = 2.48 Å, S···C(me) = 4.55 Å, OD···ON = 4.45 Å.

same structure, with the angle between the molecular dipole moment vectors about 81°, in the 50% mixture that angle is about 75°. The results indicate that although the first solvation shell is equally structured whatever the composition, at long range the 50% mixture is more structured than the other two.

For having a better view of the relative molecular orientations for the C=–OD distances in the range between 3 and 4 Å, the simulation box was scanned looking for the most statistically representative dimer formed.[61] The most frequent dimer found in that range of distance is shown in Fig. 7. Some of the geometric parameters of the dimer are reported in the figure caption.

A remarkable agreement between the site-site distances listed and the positions of the corresponding peaks in the $g(r)$ plot, Figs. 3 and 4, is to be noted. Thus, the NMF–DMSO site-site correlations in the liquid are mostly fixed for this dimer. Taking that into account, the OD–HN–N angle has been measured and is also listed in the caption of Fig. 7. It is to be noted that the O(D)–H(N) distance and the O(D)–H(N)–N angle found in that dimer agree with the values usually accepted as characterizing H-bonding.[24] Otherwise, the S–OD–N angle is about 120°, which gives an angle between the molecular dipole moment vectors equal to 170° − 120° = 50°, a value that is in quite good agreement with the value obtained in the graphic of Fig. 6. These results strongly suggest that the structure of the mixture is orientated by the presented dimer. It is observed that the site-site distances for this pair are very similar to the corresponding distances of the dimer reported previously for the 80% and 50% concentrations, reinforcing the idea that the interaction between the two molecules is not significantly dependent of the mixture concentration.

V. CONCLUSIONS

The solvation of NMF by DMSO in a NMF–DMSO liquid mixture containing 20% of NMF was investigated using a combination of neutron scattering augmented with hydrogen–deuterion substitution and EPSR simulations. The study has the purpose of investigating the structure of the NMF–DMSO mixture and the intermolecular interactions and it is believed that EPSR is a valid tool to achieve this goal. The overall fitting of the experimental data is quite good which supports the reliability of the theoretical results. The results showed indicate the formation of a strong H-bond between the O of DMSO and the amine hydrogen in noticeable agreement with experimental results reported previously.[4,5,11] The characteristics shown for this H-bond suggest that NMF might be more strongly H-bonded to DMSO than to water, or, if DMSO is added as co-solute to an aqueous solution of NMF, the water molecules H-bonded to the amine hydrogen would be delocated for it, in line with results reported previously.[9,11] Besides the O(DMSO)–H(NMF) H-bond, the results point to a secondary auxiliary S–HN H-bond, what must collaborate for the structure of the mixture.

It is worth remembering here that DMSO is strongly hydrated in water giving rise to the well known anomalies of DMSO-water mixtures at moderated DMSO concentrations, with the O of DMSO strongly H-bonded to water and a water cage around the DMSO methyl group.[45,55,62–69] Thus, it is likely that in DMSO-water medium of moderate composition, the H-bond competition of DMSO with water and NMF favors the OD–water H-bond. As a consequence, the delocation of the water molecules H-bonded to the NMF would be lower in that case, in a good parallelism with previous results.[6,7]

ACKNOWLEDGMENTS

J.M.M.C. thanks FAPESP (Fundação de Amparo à Pesquisa do Estado de São Paulo – Brazil) for supporting a stay at RAL-ISIS (Process No. 2007/07513-2) and also the ISIS Facility for the partial support of his visit.

[1]G. Rivas, J. A. Fernandez, and A. P. Minton, Proc. Natl. Acad. Sci. U.S.A. **98**, 3150 (2001).
[2]S. Dellerue, A. J. Petrescu, J. C. Smith, and M. C. Bellissent-Funel, Biophys. J. **81**, 1666 (2001).
[3]S. E. Bondos and A. Bicknell, Anal. Biochem. **316**, 223 (2003).
[4]C. Malardier-Jugroot, M. E. Johnson, D. Bowron, A. K. Soper, and T. Head-Gordon, Phys. Chem. Chem. Phys. **12**, 382 (2010).
[5]M. E. Johnson, C. Malardier-Jugroot, and T. Head-Gordon, Phys. Chem. Chem. Phys. **12**, 393 (2010).
[6]O. Almarsson and A. M. Klibanov, Biotechnol. Bioeng. **49**, 87 (1996).
[7]A. Tjernberg, N. Markova, W. J. Griffiths, and D. Hallen, J. Biomol. Screening **11**, 131 (2006).
[8]B. K. Shoichet, W. A. Baase, R. Kuroki, and B. Matthews, Proc. Natl. Acad. Sci. U.S.A. **92**, 452 (1995).
[9]T. Arakawa, Y. Kita, and S. N. Timasheff, Biophys. Chem. **131**, 62 (2007).
[10]R. V. Rariy and A. M. Klibanov, Proc. Natl. Acad. Sci. U.S.A. **94**, 13520 (1997).
[11]S. N. Timasheff, Annu. Rev. Biophys. Biomol. Struct. **22**, 67 (1993).
[12]U. Onthong, T. Megyes, I. Bako, T. Radnai, T. Grosz, K. Hermansson, and M. Probst, Phys. Chem. Chem. Phys. **6**, 2136 (2004).
[13]Y. Koga, Y. Kasahara, K. Yoshino, and K. Nishikawa, J. Solution Chem. **30**, 885 (2001).
[14]E. Bernardi and H. Stassen, J. Chem. Phys. **120**, 4860 (2004).
[15]B. Kirchner and J. Hutter, Chem. Phys. Lett. **364**, 497 (2002).
[16]R. L. Mancera, M. Chalaris, K. Refson, and J. Samios, Phys. Chem. Chem. Phys. **6**, 94 (2004).
[17]A. Vishnyakov, A. P. Lyubartsev, and A. Laaksonen, J. Phys. Chem. A **105**, 1702 (2001).
[18]M. L. Strader and S. E. Feller, J. Phys. Chem. A **106**, 1074 (2002).
[19]S. E. McLain, A. K. Soper, and A. Luzar, J. Chem. Phys. **124**, 074502 (2006).
[20]J. M. M. Cordeiro, Phys. Chem. Liq. **45**, 31 (2007).

[21]R. Notman, M. Noro, B. O'Malley, and J. Anwar, J. Am. Chem. Soc. **128**, 13982 (2006).
[22]S. Leekumjorn and A. K. Sum, Biochem. Biophys. Acta–Biomembr. **1758**, 1751 (2006).
[23]S. E. McLain, A. K. Soper, and A. Luzar, J. Chem. Phys. **127**, 174515 (2007).
[24]G. A. Geffrey, *An Introduction to Hydrogen Bonding* (Oxford University Press, New York, 1997).
[25]G. R. Desiraju and T. Steiner, *The Weak Hydrogen Bond* (Oxford University Press, Oxford, 1999).
[26]J. M. M. Cordeiro and M. A. M. Cordeiro, J. Braz. Chem. Soc. **15**, 351 (2004).
[27]J. M. M. Cordeiro and A. K. Soper, J. Phys. Chem. B **113**, 6819 (2009).
[28]A. D. Headley and J. Nam, J. Mol. Struct.: THEOCHEM **589**, 423 (2002).
[29]G. Nandini and D. N. Sathyanarayana, J. Mol. Struct.: THEOCHEM **579**, 1 (2002).
[30]J. M. M. Cordeiro, Int. J. Quantum Chem. **106**, 652 (2006).
[31]A. G. Martinez, E. T. Vilar, A. G. Fraile, and P. Martinez-Ruiz, J. Phys. Chem. A **106**, 4942 (2002).
[32]F. Hammami, S. Nasr, and M. C. Bellisent-Funel, J. Chem. Phys. **122**, 064505 (2005).
[33]F. Hammami, S. Nasr, M. Oumezzine, and R. Cortes, Biomol. Eng. **19**, 201 (2002).
[34]G. G. Almeida and J. M. M. Cordeiro, J. Braz. Chem. Soc. **22**, 2178 (2011).
[35]J. M. M. Cordeiro and A. K. Soper, Chem. Phys. **381**, 21 (2011).
[36]J. M. M. Cordeiro and A. R. S. A. Bosso, J. Mol. Liq. **154**, 36 (2010).
[37]E. C. Hulme, A. K. Soper, S. E. McLain, and J. L. Finney, Biophys. J. **91**, 2371 (2006).
[38]P. E. Mason, G. W. Neilson, J. E. Enderby, M. L. Saboungi, and J. W. Brady, J. Phys. Chem. B **109**, 13104 (2005).
[39]P. E. Mason, G. W. Neilson, J. E. Enderby, M. L. Saboungi, and J. W. Brady, J. Phys. Chem. B **110**, 2981 (2006).
[40]S. E. McLain, A. K. Soper, and A. Watts, J. Phys. Chem. B **110**, 21251 (2006).
[41]S. E. McLain, A. K. Soper, A. E. Terry, and A. Watts, J. Phys. Chem. B **111**, 4568 (2007).
[42]A. Botti, F. Bruni, S. Imberti, M. A. Ricci, and A. K. Soper, J. Mol. Liq. **117**, 77 (2005).
[43]A. Botti, F. Bruni, S. Imberti, M. A. Ricci, and A. K. Soper, J. Mol. Liq. **117**, 81 (2005).
[44]A. K. Soper and J. L. Finney, Phys. Rev. Lett. **71**, 4346 (1993).
[45]A. K. Soper and A. Luzar, J. Phys. Chem. **100**, 1357 (1996).
[46]A. K. Soper, Chem. Phys. **258**, 121 (2000).
[47]S. E. McLain, C. J. Benmore, J. E. Siewenie, J. Urquidi, and J. F. C. Turner, Angew. Chem., Int. Ed. **43**, 1952 (2004).
[48]J. L. Finney, D. T. Bowron, and A. K. Soper, J. Phys.: Condens. Matter **12**, A123 (2000).
[49]V. F. Sears, Neutron News **3**, 26 (1992).
[50]A. K. Soper, Mol. Phys. **99**, 1503 (2001).
[51]A. K. Soper, Phys. Rev. B **72**, 104204 (2005).
[52]S. E. McLain, A. K. Soper, and A. Watts, Eur. Biophys. J. Biophys. Lett. **37**, 647 (2008).
[53]A. K. Soper, *GudrunN and GudrunX: Programs for correcting raw neutron and X-ray diffraction data to differential scattering cross section*, RAL Technical Report No. -RAL-TR-2011-013, Didcot, UK 2011, also see http://epubs.stfc.ac.uk/.
[54]A. K. Soper and E. M. Barney, J. Appl. Cryst. **44**, 714 (2011).
[55]A. Luzar and D. Chandler, J. Chem. Phys. **98**, 8160 (1993).
[56]M. P. Allen and D. J. Tildesley, *Computer Simulation of Liquids* (Oxford University Press, Oxford, 1987).
[57]D. Frenkel and B. Smith, *Understanding Molecular Simulation: From Algorithms to Applications* (Academic, New York, 1996).
[58]L. C. G. Freitas, J. Braz. Chem. Soc. **20**, 1541 (2009).
[59]J. M. M. Cordeiro, Z. Naturforsch. A **54**, 311 (1999).
[60]M. A. M. Cordeiro, W. P. Santana, R. Cusinato, and J. M. M. Cordeiro, J. Mol. Struct.: THEOCHEM **759**, 159 (2006).
[61]V. Sayle, Molecular Visualization Program, RASMOL v2.5, Glaxo Research and Development, Greenford, Middlesex, 1999.
[62]I. A. Borin and M. S. Skaf, J. Chem. Phys. **110**, 6412 (1999).
[63]D. Laria and M. S. Skaf, J. Chem. Phys. **111**, 300 (1999).
[64]M. S. Skaf, J. Phys. Chem. **103**, 10719 (1999).
[65]M. S. Skaf and S. M. Vechi, J. Chem. Phys. **119**, 2181 (2003).
[66]S. S. N. Murthy, Cryobiology **36**, 84 (1998).
[67]A. Luzar, A. K. Soper, and D. Chandler, J. Chem. Phys. **99**, 6836 (1993).
[68]A. Luzar, Faraday Discuss. **103**, 29 (1996).
[69]J. T. Cabral, A. Luzar, J. Teixeira, and M. C. Bellissent-Funel, J. Chem. Phys. **113**, 8736 (2000).